J|A|C|S
COMMUNICATIONS

Published on Web 03/17/2007

Gold-Coated Transition-Metal Anion $[Mn_{13}@Au_{20}]^-$ with Ultrahigh Magnetic Moment

Jinlan Wang,[†] Jaeil Bai,[‡] Julius Jellinek,[§] and Xiao Cheng Zeng*,[‡]

Department of Physics, Southeast University, Nanjing, 210096, P. R. China, Department of Chemistry and Nebraska Center for Materials and Nanoscience, University of Nebraska, Lincoln, Nebraska 68588, and Chemistry Division, Argonne National Laboratory, Argonne, Illinois 60439

Received September 5, 2006; E-mail: xczeng@phase2.unl.edu

A variety of intriguing magnetic properties have been uncovered in transition-metal (TM) clusters with fewer than $\sim 10^2$ atoms.[1] For example, enhanced magnetic moments have been observed in small clusters of iron.[1a] Ferromagnetic or ferrimagnetic ordering has been detected in clusters of rhodium, chromium, and manganese, although these elements are nonmagnetic or antiferromagnetic in bulk quantities.[1c,2] Magnetic features have also been explored in bimetallic clusters.[3−6] A particularly interesting case is that of small core/shell systems built of elements that exhibit different magnetic features in the regime of small sizes.[7−10] In this Communication we report a novel gold-coated icosahedral TM cluster $[Mn_{13}@Au_{20}]^-$ with a magnetic moment predicted to be *an order of magnitude* higher than that of the bare (core) Mn_{13}^-.

We consider an idealized gold coating in the form of an icosahedral Au_{20} cage whose structure is similar to that of the icosahedral C_{20} fullerene. Because of the strong relativistic effect, small gold clusters exhibit structures and properties[11−14] that are dramatically different from those of other coinage metal (e.g., copper[14]) clusters. It is interesting that whereas the I_h hollow cage structure of Au_{12}^- as well as its neutral counterpart is unstable, the icosahedral core/shell clusters $[M@Au_{12}]^-$, M = Ta, W, Mo, V, Nb, are highly stable.[9] The I_h Au_{12} cage can host one endohedral atom only. The I_h Au_{20} cage is larger and can accommodate a small cluster. In similarity to the I_h Au_{12} cage, the bare I_h Au_{20} cage is unstable. By putting a highly stable TM cluster, such as the I_h Co_{13}^- or Mn_{13}^- into it, one can stabilize the gold cage as well.

The calculations are carried out using density functional theory (DFT) with the Perdew, Burke, and Ernzerhof (PBE) functional.[15] Scalar relativistic pseudopotentials and double numerical (DND) basis sets that included *d* polarization functions, as implemented in the DMol[3] package,[16] are employed. The accuracy of the methodology is examined by first computing the properties of neutral Co_{13} and Mn_{13}. For Co_{13}, the lowest-energy spin (more precisely, S_z) states are 29 and 31 μ_B. They correspond to I_h structures and are essentially degenerate. Both are consistent with the experimental estimate of more than 2.0 μ_B/atom.[17] For Mn_{13}, the lowest-energy structure is a distorted icosahedron (C_{5v}) with a total S_z value of 3 μ_B. These results are consistent with those of earlier experimental[2] and theoretical[18] studies. In the latter study, Jackson and co-workers[18] have examined all possible 4096 independent arrangements of the atomic spin for Mn_{13}. The consistency in the determination of the lowest-energy spin state for Mn_{13} from two different theoretical approaches is very encouraging.

The search for the lowest-energy states of the bare Mn_{13}^- and Co_{13}^- and gold-coated $[Mn_{13}@Au_{20}]^-$ and $[Co_{13}@Au_{20}]^-$ are performed over broad ranges of S_z values. Thus, for Mn_{13}^- and $[Mn_{13}@Au_{20}]^-$ we considered all values from 2 to 64 μ_B, and for Co_{13}^- and $[Co_{13}@Au_{20}]^-$, we considered all values from 2 to 38 μ_B. We found that the optimized geometries of the clusters are very close to the I_h structure (within 0.06 Å tolerance). Hence, the computation for different spin states were performed imposing the I_h symmetry to reduce the computational effort. Taking into account that the Mn bulk phase is antiferromagnetic, symmetry-broken implementations (which correspond to antiparallel ordering of the atomic spin) were also considered for Mn_{13}^- and $[Mn_{13}@Au_{20}]^-$ with S_z = 2−52 μ_B. The stability of the lowest energy structures/states obtained was confirmed through the normal-mode analysis. The optimized geometry of the $[TM_{13}@Au_{20}]^-$, TM = Mn and Co, clusters is depicted in Figure 1. The relative energies of the different spin-multiplicity states of the bare and gold-coated Mn_{13}^- and Co_{13}^- are shown in Figure 2. The HOMO−LUMO gap, nearest-neighbor distances, and local atomic S_z values for the most stable states of the clusters are presented in Table 1. Additional data on the total energies, relative energies, binding energies, and HOMO−LUMO gaps of the different spin states of the clusters are presented in Supporting Information (Tables S1−S4).

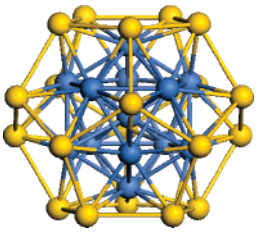

Figure 1. Optimized geometry of $[TM_{13}@Au_{20}]^-$, TM = Mn and Co. Blue represents the TM core, while yellow depicts the gold shell.

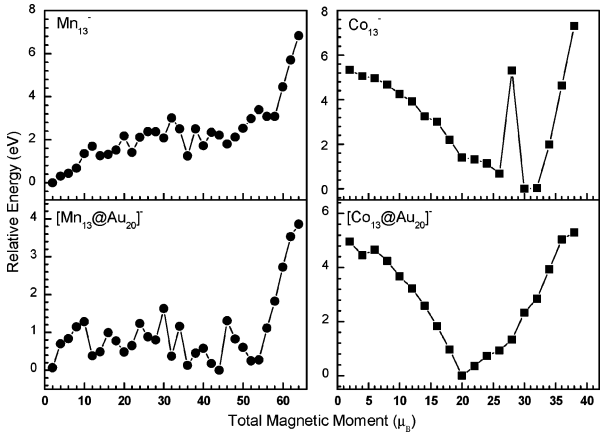

Figure 2. Energies of TM_{13}^- and $[TM_{13}@Au_{20}]^-$, TM = Mn and Co, in different spin states referred to the respective lowest-energy states.

[†] Southeast University.
[‡] University of Nebraska.
[§] Argonne National Laboratory.

10.1021/ja0664234 CCC: $37.00

Table 1. The Total Magnetic Moment (S_2), the HOMO−LUMO Gap (Δ), the Bond Length (R in Å), Local Magnetic Moment (S in μ_B) on Each Atom of the Most Stable Structure of TM_{13}^- and $[TM_{13}@Au_{20}]^-$, TM = Mn and Co (See the Text for Details)

system	S_z (μ_B)	Δ (eV)	R_{TM} (surf−surf)	R_{TM} (surf−core)	R_{Au-TM}(surf)	R_{Au-TM} (core)	R_{Au-Au}	S_{TM} (surf)	S_{TM} (core)	S_{Au}
Mn_{13}^-	2	0.215	2.619	2.489				3.892, −4.109	1.212	
$[Mn_{13}@Au_{20}]^-$	44	0.248	2.847	2.706	2.611	4.441	2.973	3.949, −3.877	2.679	0.088
Co_{13}^-	30	0.025	2.321	2.441				2.347	1.834	
$[Co_{13}@Au_{20}]^-$	20	0.338	2.363	2.486	2.606	4.291	2.892	1.607	1.848	−0.057

The lowest energy configuration of $[Mn_{13}@Au_{20}]^-$ is a slightly distorted icosahedral structure (C_{5v}) with a very large total S_z of 44 μ_B. The magnetic ordering is in a ferrimagnetic arrangement of which 1 surface Mn atom is antiparallel to the rest 11 ones with the atomic spins of −3.877 and 3.949 μ_B, and the core atom possesses the local moment of 2.679 μ_B. The low spin state with the total S_z of 2 μ_B is found to be only 0.071 eV higher in energy. More high spin states such as the total S_z of 36, 42, 52, and 54 μ_B are found as deep minima with 0.133, 0.182, 0.253, and 0.277 eV higher in energy than the ground state. For the case of $S_z = 2$ μ_B, six surface Mn atoms are antiparallel to the rest six ones with the atomic moment of 3.927 and −4.104 μ_B, respectively. The core Mn atom possesses a moment of 3.066 μ_B. As for the case of $S_z =$ 36 μ_B, two symmetric apex Mn atoms are antiparallel (−3.770 μ_B) to the rest Mn atoms (3.981 μ_B for the surface atoms and 2.575 μ_B for the core atom). All the Mn atoms are parallel and the local moments of Mn atom are around 4.0 μ_B in the case of $S_z = 52$ and 54 μ_B. In contrast, the bare Mn_{13}^- favors a ferrimagnetic ordering[18] of the local atomic spins with a net total value of 2 μ_B (cf. Table 1). The lowest ferromagnetic state of Mn_{13}^- is with a total S_z of 52 μ_B, and its energy is 2.980 eV higher above the ground state.

Whereas the geometric configuration of $[Co_{13}@Au_{20}]^-$ is similar to that of $[Mn_{13}@Au_{20}]^-$, its magnetic behavior is very different. Its preferred total S_z value is 20 μ_B, 33% lower than the optimal value (30 μ_B) for the bare Co_{13}^-. Interestingly, the Co atoms are ferromagnetically ordered in both the bare and the gold-coated Co_{13}^-, although the atomic S_z in the bare cluster are quite a bit larger (2.35 vs 1.61 μ_B for surface atoms and 1.83 vs 1.85 μ_B for the core atom). A further reduction of the total S_z of $[Co_{13}@Au_{20}]^-$ is caused by the antiparallel ordering of the moments of all the Au atoms (0.057 μ_B per Au) with respect to the moments of the Co atoms (cf. Table 1).

The differences in the magnetic properties of $[Mn_{13}@Au_{20}]^-$ and $[Co_{13}@Au_{20}]^-$ may reflect the differences in the relative magnitudes of their interatomic distances. The data in Table 1 indicate that in $[Mn_{13}@Au_{20}]^-$ the element-specific nearest-neighbor distances R follow the order R(surf-surf Mn) > R(surf-core Mn) > R(surf Mn-Au), whereas in $[Co_{13}@Au_{20}]^-$ this order is reversed, R(surf-surf Co) < R(surf-core Co) < R(surf Co-Au). The Mn−Mn bond length in $[Mn_{13}@Au_{20}]^-$ is by ∼9% larger than in the bare Mn_{13}^-. Previous DFT studies indicated that reduction in the bond lengths leads to a transition from ferromagnetic to antiferromagnetic ordering in small iron clusters.[18] For $[Co_{13}@Au_{20}]^-$, the bond length of Co−Co is nearly the same as that in the bare Co_{13}^-. A possible reason for the decrease of magnetic moment in $[Co_{13}@Au_{20}]^-$ is that the gold cage has an attenuation effect on the magnetism of highly magnetic clusters. We speculate that a similar decrease might occur in the core/shell $Fe_{13}@Au_{20}$. In fact, in a previous study of Co−Cu bimetallic clusters, we have observed similar attenuated magnetic behavior in Co_7Cu_{11} with the pentagonal bipyramid Co_7 surrounded by 11 Cu atoms.[19]

In summary, we have presented results of DFT computations which show that coating magnetic clusters with gold can both enhance (as in the case of $[Mn_{13}@Au_{20}]^-$) and attenuate (as in the case of $[Co_{13}@Au_{20}]^-$) the net magnetic moment of the clusters. The degree of magnetic enhancement for $[Mn_{13}@Au_{20}]^-$ (44 μ_B) as well as the cluster's bistability at both low (2 μ_B) and high (44 μ_B) spin states suggests that the gold-coated manganese clusters may be good prototype systems for nanomagnetism applications.

Acknowledgment. This work was supported by National Nature Science Foundation of China (No. 10604013) and the Teaching and Research Foundation for the Outstanding Young Faculty of Southeast University (J.W.); by the Office of Basic Energy Sciences, Division of Chemical Sciences, Geosciences, and Biosciences, U.S. Department of Energy (No. DE-AC-02-06CH11357) and NERSC (J.J.); and by the Office of Basic Energy Sciences (Grant DE-FG02-04ER46164), National Science Foundation (CHE and MRSEC), the Nebraska Research Initiative, and the UNL Research Computing Facility (X.C.Z.).

Supporting Information Available: Complete ref 3; the total energy, relative energies, binding energies, as well as the HOMO−LUMO gaps of the clusters. This material is available free of charge via the Internet at http://pubs.acs.org.

References

(1) (a) Billas, I. M. L.; Chatelain, A.; de Heer, W. A. *J. Mag. Mag. Mater.* **1997**, *168*, 64. (b) Alonso, J. A. *Chem. Rev.* **2000**, *100*, 637. (c) Bloomfield, L. A.; Deng, J.; Zhang, H.; Emmert, J. W. *Proc. Int. Symp. Cluster. Nanostruct. Interfaces* **2000**, 131.
(2) Knickelbein, M. B. *Phys. Rev. B* **2004**, *70*, 014424.
(3) Bansmann, J.; et al. *Surf. Sci. Rep.* **2005**, *56*, 189.
(4) (a) Janssens, E.; Tanaka, H.; Neukermans, S.; Silverans, R.; Lievens, P. *Phys. Rev. B* 2004, *69*, 085402. (b) Neukermans, S.; Janssens, E.; Tanaka, H.; Silverans, R. E.; Lievens, P. *Phys. Rev. Lett.* **2003**, *90*, 033401.
(5) Torres, M. B.; Fernandez, E. M.; Balbas, L. C. *Phys. Rev. B* **2005**, *71*, 155412.
(6) Nicolas, G.; Dorantes-Davila., J.; Pastor, G. M. *Phys. Rev. B* **2006**, *74*, 014415.
(7) Lin, J.; Zhou, W. L.; Kumbhar, A.; Wiemann, J.; Fang, J. Y.; Carpenter, E. E.; O'Connor, C. J. *J. Solid State Chem.* **2001**, *159*, 26.
(8) Guevara, J.; Llois, A. M.; Weissmann M. *Phys. Rev. Lett.* **1998**, *81*, 5306.
(9) (a) Pyykkö, P.; Runeberg N, *Angew Chem., Int. Ed.* **2002**, *41*, 2174. (b) Zhai, H. J.; Li, J.; Wang, L. S. *J. Chem. Phys.* **2004**, *121*, 8329. (c) Gao, Y; Bulusu, S.; Zeng, X. C. *ChemPhysChem* **2006**, *7*, 2275. (d) Walter, M.; Hakkinen, H. *Phys. Chem. Chem. Phys.* **2006**, 5407.
(10) Sun, Q.; Kandalam, A. K.; Wang, Q.; Jena, P.; Kawazoe, Y.; Marquez, M. *Phys. Rev. B* **2006**, *73*, 134409.
(11) (a) Furche, F.; Ahlrichs, R.; Weis, P.; Jacob, C.; Glib, S.; Bierweiler, T.; Kappes, M. M. *J. Chem. Phys.* **2002**, *117*, 6982. (b) Hakkinen, H.; Yoon, B.; Landman, U.; Li, X.; Zhai, H. J.; Wang, L. S. *J. Phys. Chem. A* **2003**, *107*, 6168. (c) Bulusu, S.; Li, X.; Wang, L.-S.; Zeng, X. C. *Proc. Natl. Acad. Sci. U.S.A.* **2006**, *103*, 8326.
(12) Garzon, I. L.; Michaelian, K.; Beltran, M. R.; Posada-Amarillas, A.; Ordejon, P.; Artacho, E.; Sanchez-Portal, D.; Soler, J. M. *Phys. Rev. Lett.* **1998**, *81*, 1600.
(13) (a) Pyykkö, P. *Angew. Chem., Int. Ed.* **2004**, *43*, 4412. (b) Li, J.; Li, X.; Zhai, H.; Wang, L. *Science* **2003**, *299*, 864. (c) Fernandez, E. M.; Soler, J. M.; Balbas, L. C. *Phys. Rev. B* **2006**, *73*, 235433.
(14) (a) Wang, J. L.; Wang, G. H.; Zhao, J. J. *Chem. Phys. Lett.* **2003**, *380*, 716. (b) Yang, M.; Jackson, K. A.; Koehler, C.; Frauenheim, T.; Jellinek, J. *J. Chem. Phys.* **2006**, *124*, 024308.
(15) Perdew, J. P.; Burke, K.; Ernzerhof, M. *Phys. Rev. Lett.* **1996**, *77*, 3865.
(16) DMol^3 is a density functional theory program distributed by Accelrys, Inc. Delley, B. *J. Chem. Phys.* **1990**, *92*, 508.
(17) Xu, X. S.; Yin, S. Y.; de Heer, W. A. *Phys. Rev. Lett.* **2005**, *95*, 237209.
(18) Bobadova-Parvanova, P.; Jackson, K. A.; Srinivas, S; Horoi, M. *Phys. Rev. B* **2002**, *66*, 195402.
(19) Wang, J. L.; Wang, G. H.; Chen, X. S.; Lu, W.; Zhao, J. J. *Phys. Rev. B* **2002**, *66*, 014419.

JA0664234